Earth and Planetary Science Letters 541 (2020) 116290

Contents lists available at ScienceDirect

Earth and Planetary Science Letters

www.elsevier.com/locate/epsl

Low-temperature oceanic crust alteration and the isotopic budgets of potassium and magnesium in seawater

Danielle P. Santiago Ramos [a,*], Laurence A. Coogan [b], Jack G. Murphy [a], John A. Higgins [a]

[a] Department of Geosciences, Princeton University, Princeton, NJ 08544 USA
[b] School of Earth and Ocean Sciences, University of Victoria, Victoria, BC, Canada

ARTICLE INFO

Article history:
Received 29 August 2019
Received in revised form 17 March 2020
Accepted 15 April 2020
Available online 4 May 2020
Editor: L. Derry

Keywords:
low-temperature oceanic crust alteration
potassium isotopes
magnesium isotopes
lithium isotopes
global potassium cycle
global magnesium cycle

ABSTRACT

Low-temperature (<100 °C) alteration of oceanic crust plays an important role in determining the chemical composition of the oceans. Although a major sink of seawater potassium, little is known about the effects of low-temperature basalt alteration on the potassium isotopic composition of seawater (δ^{41}K∼0‰), which is ∼0.50‰ enriched relative to bulk silicate Earth (BSE, δ^{41}K= -0.54‰). Here, we present a suite of isotopic systems (δ^{41}K, δ^{26}Mg, δ^{7}Li, ^{87}Sr/^{86}Sr) and major/minor elements in bulk rock, veins and mineral separates from the upper volcanic section of Cretaceous (Troodos ophiolite) and Jurassic (Ocean Drilling Program Hole 801C) oceanic crust. We use these data to estimate the K isotopic fractionation associated with low-temperature oceanic crust alteration and provide new constraints on the role of this process in the global geochemical cycles of Mg and K in seawater. We find that hydrothermally altered basalts from the Troodos ophiolite and ODP Hole 801C, most of which are enriched in K relative to the unaltered glass compositions, have δ^{41}K values both higher and lower than BSE, ranging from +0.01‰ to -1.07‰ (n=83) and +0.04‰ to -0.88‰ (n=17), respectively. Average δ^{41}K values of bulk-rock samples from Troodos and Hole 801C are indistinguishable from each other at ∼-0.50‰, indicating that low-temperature basalt alteration is a sink of ^{39}K from seawater, and explaining, in part, why seawater has a higher ^{41}K/^{39}K than BSE. In contrast to K, average δ^{26}Mg values for both Troodos (∼0.00‰) and Hole 801C (∼0.20‰) indicate that altered oceanic crust (AOC) is a sink of ^{26}Mg from seawater, likely contributing to the light δ^{26}Mg composition of seawater (∼-0.8‰) relative to BSE (∼-0.2‰). We observe isotopically heavy δ^{26}Mg values in basalt samples characterized by small to no changes in bulk Mg content, consistent with extensive isotopic exchange of Mg between seawater and oceanic crust during low-temperature oceanic crust alteration. Finally, we find that variability in δ^{7}Li and δ^{41}K across three sites in the Troodos ophiolite can be explained by different styles of alteration that appear to be related to the timing of sedimentation and its effects on chemical and isotopic exchange between seawater and oceanic crust.

1. Introduction

Reconstructions of ancient seawater chemistry from fluid inclusions in marine halite have suggested that, unlike other major ions (e.g. Ca^{2+}, Mg^{2+}, SO_4^{2-}), concentrations of K^+ in the ocean have apparently remained at ∼10 mM over the last 600 My (Lowenstein et al., 2001; Horita et al., 2002). These observations suggest that strong feedbacks in the global K cycle may have acted to maintain constant seawater K^+ in face of large changes in input and output fluxes (Demicco et al., 2005; Coogan and Gillis, 2013).

Despite being a major seawater cation, the global seawater potassium cycle remains poorly understood. Potassium is delivered to the oceans from the breakdown of silicate minerals during continental weathering, and via high-temperature (>150 °C; e.g. Seyfried and Bischoff, 1979; James et al., 2003) leaching of oceanic crust along mid-ocean ridges (Kronberg, 1985; Spencer and Hardie, 1990; Demicco et al., 2005). Scavenging of seawater K happens via the formation of authigenic silicates during both marine sedimentary diagenesis and alteration of oceanic crust under low-temperature conditions (<100 °C; e.g. Alt and Teagle, 2003; Coogan et al., 2017). In some of these authigenic silicate reactions, the CO_2 initially consumed from the breakdown of continental/marine silicates is returned to the atmosphere-ocean system during secondary mineral formation (i.e. reverse weathering; Michalopoulos and Aller, 1995). As a result, the formation of authigenic marine

* Corresponding author.
E-mail address: dpramos@alumni.princeton.edu (D.P. Santiago Ramos).

https://doi.org/10.1016/j.epsl.2020.116290
0012-821X/

silicates represents a potentially powerful and understudied control on Earth's CO_2-thermostat (e.g. Dunlea et al., 2017).

The development of high-precision methods for K isotope ratio measurements ($^{41}K/^{39}K$; Li et al., 2016; Wang and Jacobsen, 2016; Morgan et al., 2018; Hu et al., 2018; Chen et al., 2019) has revealed that the $^{41}K/^{39}K$ of seawater is ~0.5‰ higher than that of bulk silicate Earth (BSE), a difference which must be due to K isotope fractionation during (a) continental weathering (Li et al., 2019), (b) high-temperature hydrothermal alteration, and/or (c) removal of K from seawater into authigenic minerals. Santiago Ramos et al. (2018) demonstrated that marine authigenic clay formation is a sink of ^{39}K from seawater, though the magnitude of the fractionation depends on the type of silicate forming and sedimentation rates. In addition, a recent K isotope study of continental weathering showed that ^{39}K is removed during secondary clay formation, resulting in a riverine $\delta^{41}K$ value higher than BSE (Li et al., 2019). In contrast, K isotope measurements of the Bay of Islands ophiolite indicate little to no fractionation of K isotopes during K uptake in altered oceanic crust (AOC; Parendo et al., 2017). However, this result is based on a handful (n=6) of measurements from samples deeper in the ophiolite and may not be representative of the average K-isotopic fractionation from K uptake in the upper volcanics, the section of AOC associated with the most extensive seawater-K addition (e.g. Bednarz and Schmincke, 1989).

Low-temperature oceanic crust alteration has also been proposed as a major sink of seawater Mg and Li, and an important but uncertain component of the isotopic mass balance of these elements in seawater. For example, Higgins and Schrag (2015) and Gothmann et al. (2017) invoked a decrease in the Mg sink in low-temperature hydrothermal systems to explain both the rise in seawater Mg/Ca and the small change in $\delta^{26}Mg$ of seawater over the Cenozoic. More recently, Huang et al. (2018), using measurements of the Mg-isotopic composition of AOC from ODP Hole 801C, argued that the $\delta^{26}Mg$ of modern seawater is consistent with a low-temperature hydrothermal sink that accounts for 12% of the riverine Mg flux. Estimates based on the $\delta^{26}Mg$ composition of low-temperature hydrothermal fluids indicate a much larger Mg flux into altered oceanic crust, accounting for up to 40% of the riverine influx (Shalev et al., 2019). In the case of Li, while modern seawater composition is consistent with a low-temperature hydrothermal Li sink equal to 30% of the total inputs (Misra and Froelich, 2012), published $\delta^{7}Li$ values of altered basalts from Troodos suggest that the hydrothermal Li sink was much larger in the Cretaceous (Coogan et al., 2017).

Here, we investigate how oceanic crust altered at low temperatures affects the K- and Mg-isotopic composition of seawater by focusing on the upper volcanics (~500 m) of the Cretaceous Troodos ophiolite (~91.6 Ma) and Jurassic Ocean Drilling Program (ODP) Hole 801C (~167 Ma). We estimate isotopic fractionation during low-temperature basalt-seawater exchange by calculating average values for $\delta^{41}K$ (weighted by K/Ti ratio) and $\delta^{26}Mg$ (weighted by Mg/Ti ratio) from both Troodos and ODP Hole 801C bulk-rock samples. Our results suggest that K uptake during low-temperature oceanic crust alteration is associated with fractionation of K isotopes, with alteration products enriched in ^{39}K compared to seawater. In contrast, we find that AOC constitutes a sink of heavy magnesium (^{26}Mg) from seawater, in line with previous results (Huang et al., 2018; Shalev et al., 2019). Our study also indicates a decoupling between elemental and isotopic cycling of Mg during low-temperature oceanic crust alteration, as we observe significant Mg isotopic resetting accompanied by small to no changes in Mg contents of most AOC samples analyzed here. Finally, we explore mechanisms underlying the observed variability in $\delta^{41}K$ values within the Troodos ophiolite using three sections of upper volcanics that have experienced different histories of low-temperature hydrothermal alteration.

2. Description of study sites

The Troodos ophiolite constitutes a complete section of oceanic lithosphere, formed during a period of seafloor spreading in a supra-subduction zone setting in the Tethys Ocean (Moores et al., 1984). Troodos volcanic sequence has variable thickness and can be divided into two compositionally distinct units. The Upper Lava sequence contains highly depleted arc tholeiites of boninitic affinity with low Ti contents, while the Lower Lavas are composed of island-arc tholeiitic basalts with higher Ti contents (Malpas and Williams, 1991), though these are intermixed at some crustal levels. In order to track compositional changes during alteration, we normalize major element concentrations to that of Ti, since the latter is virtually immobile during low-temperature basalt-seawater reactions. Although Ti contents vary across these volcanic units, K/Ti ratios of unaltered glass show a small range (0.15-1.25 g/g) and average at 0.40 $\pm$0.18 (1σ; Regelous et al., 2014; Coogan and Gillis, 2018). In contrast, glass Mg/Ti ratios are quite variable (1.11-16.75 g/g), likely resulting from magmatic differentiation.

Troodos ophiolite samples include 90 whole rocks and 3 mineral separates from six sites in the upper-volcanic sequence and one (Klirou) in the basal group (Fig. 1B). The mineral samples are all void-filling celadonites that were easily separated from the host rock (Coogan et al., 2017); although also important for the K budget of these altered basalts, K-feldspar separates were not included here since it typically appears as a fine-grained, replacement phase that is difficult to isolate. Three upper-volcanic sites (Akaki, Politico, and Onophrious) were selected to explore the effects of sedimentation on the chemical/isotopic exchange between seawater and oceanic crust (e.g. Elderfield et al., 1999). Onophrious represents a paleo-topographic low, is rich in sheet-flow lavas, and was sedimented shortly after crustal formation. In contrast, Politico and Akaki correspond to flat paleo-seafloor areas, are predominantly composed of pillow basalts, and did not start accumulating sediment until ~20 Myr after crustal accretion (Coogan et al., 2017). Politico and Onophrious samples come from outcrop exposures, whereas Akaki samples were acquired from Cyprus Crustal Study Project drill sites CY1/CY1a.

Our sample suite also includes bulk-rock (n=17) and vein (n=6) specimens from Ocean Drilling Program (ODP) Hole 801C (Leg 185), a ~474-meter section of Jurassic oceanic crust (Plank et al., 2000). The site is located in the Pacific Ocean (18°38.538′N, 156°21.588′E; Fig. 1A), consists of eight lithological units, and is covered by ~0.5 km of sediment (Plank et al., 2000). Apart from the upper alkali basalts (unit I), Hole 801C samples have N-MORB compositions with a common magmatic source (Plank et al., 2000). Measured K/Ti ratios of unaltered rocks vary between 0.01 and 0.11 g/g, and Mg/Ti ratios range from 1.94 to 6.11 g/g (Fisk and Kelley, 2002; Alt and Teagle, 2003). Secondary mineralogy is mainly composed of low-K saponite, calcite, high-K celadonite, iron-oxyhydroxides and trace pyrite (Plank et al., 2000; Alt and Teagle, 2003). These alteration minerals are typical products of low-temperature (<100 °C) basalt-seawater interaction and are similar to those observed in other drilled upper-crustal sections as well as in the Troodos ophiolite. Our 801C sample set includes pillows and sheet flows from units IV, VI and VIII (Supp. Table S1).

3. Methods

3.1. Mineralogy

Mineral quantification of 42 bulk samples from the Troodos ophiolite was carried out by Qmineral Analysis and Consulting, Belgium. Homogenized dry powders (0.2-1.0 g) were combined with 10% (by mass) of an internal standard material (ZnO) and ground

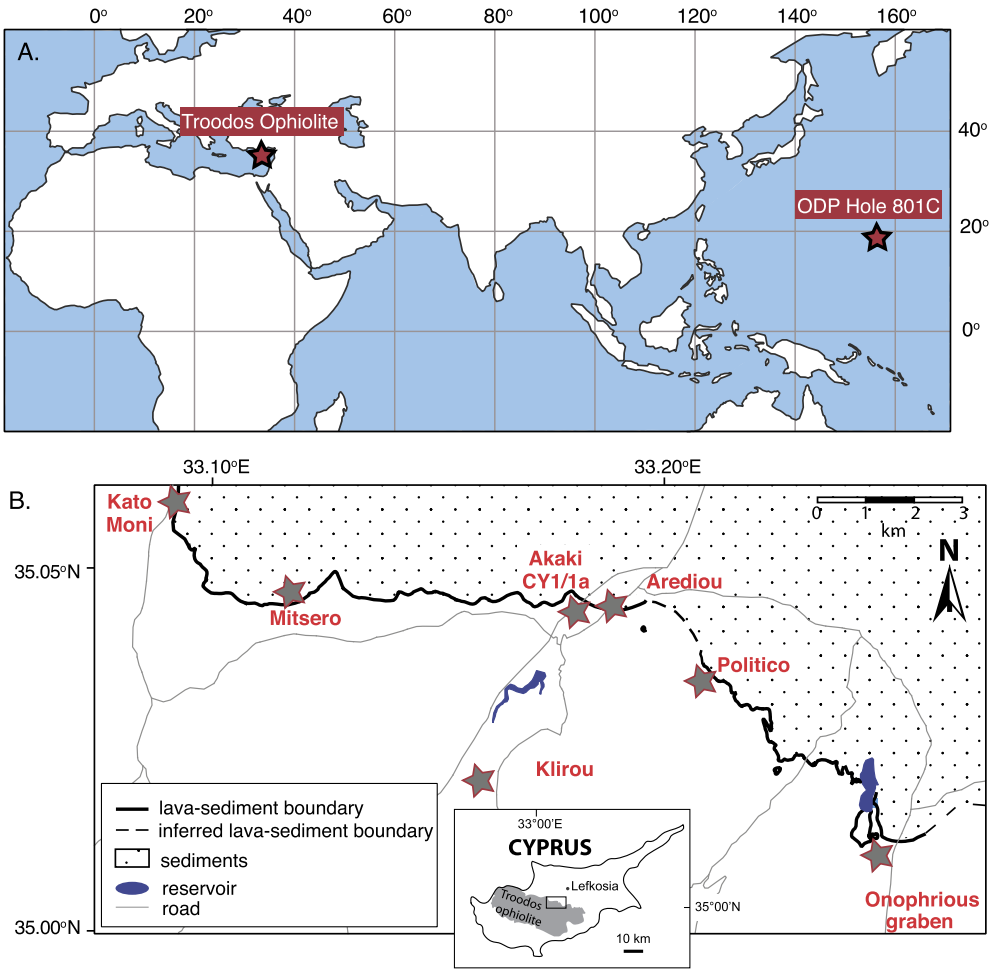

Fig. 1. Location of study sites. (A) Global map indicating locations for the Troodos ophiolite and Ocean Drilling Program (ODP) Hole 801C; (B) Detailed map of the Troodos ophiolite showing all sites analyzed in this study, along with important lithological boundaries. Map is adapted from Coogan et al. (2017).

in ethanol. Samples were measured by X-ray diffraction in a Bruker D8 diffractometer with CuKα radiation, equipped with a Lynxeye XE-T detector. Mineral quantification was performed through a combination of an in-house method and the Rietveld method, using the Inorganic Crystal Structure Database (ICSD).

3.2. Sample digestion and major/minor element analyses

Approximately 50 mg of rock/mineral powder was weighed into 15 mL Teflon beakers for a 3-step HF-HNO_3-HCl hotplate digestion in a laminar flow hood (Supp. Info. A). Each digestion batch included ~19 unknowns and one basalt standard (BCR-2). Major/minor element analyses were carried out at Princeton University using a quadrupole inductively coupled plasma mass spectrometer (Thermo Scientific iCap Q). Concentrations and elemental ratios were determined using externally calibrated standards (Supp. Info. B). Replicate analyses of BCR-2 (n=10) indicate that our results are accurate to within 10% of the expected values (Supp. Table S5) and signal drift was mostly lower than 10% (Supp. Info. B).

3.3. Ion chromatography and mass spectrometry

Cations were purified using either an automated high-pressure ion chromatography (IC) system (K, Mg, Li) or traditional gravity columns (Sr). The IC methods utilized here followed those previously described in Morgan et al. (2018) and Santiago Ramos et al. (2018) for K, and in Husson et al. (2015) for Mg; Li and Sr purification methods are discussed in detail in Supp. Info. C-D. The accuracy of our chromatographic methods was verified by purifying and analyzing external standards (SRM70b for K, Cambridge-1 for Mg, L-SVEC for Li, BCR-2 for Sr, and modern seawater) alongside unknown samples. As this is the first study utilizing an IC for Li isotope analyses, we performed a series of tests to establish both the accuracy and precision of the method (Supp. Info. E), and reproduced δ^7Li values of 10 samples reported in Gillis et al. (2015) and Coogan et al. (2017) (Supp. Table S2).

Purified aliquots of K, Mg, Li, and Sr were analyzed in 2% HNO_3 for their isotopic compositions on a Thermo Scientific Neptune Plus multi-collector inductively coupled plasma mass spectrometer (MC-ICP-MS) at Princeton University, using previously published methods for Mg and K (Fantle and Higgins, 2014; Morgan et al., 2018), and the protocols detailed in the Supplementary Information for Li and Sr. K, Mg, and Li isotopes are reported in delta notation (δ^{41}K, δ^{26}Mg, δ^7Li) relative to international standards (seawater, DSM-3, and L-SVEC, respectively) and $^{87}Sr/^{86}Sr$ ratios are normalized to NBS 987. Other standards have been used for K isotopic data normalization (e.g. SRM 3141a, Suprapur KNO_3), leading to small differences in reported δ^{41}K values for seawater. To account for that, we have also provided δ^{41}K values normalized to SRM 3141a (Supp. Tables S1–S2) in order to facilitate interlaboratory data comparison. We did this by simply shifting our seawater-normalized values by 0.12‰, which corresponds to the difference between our seawater average (-0.02‰) and the average $\delta^{41}K_{SRM3141a}$ composition of seawater (0.10‰) based on values reported in Li et al. (2016) and Hu et al. (2018). We stress that,

despite differences in the adopted K isotope scale, data reported from different labs are indistinguishable within uncertainties, as has been demonstrated in Hu et al. (2018) and Chen et al. (2019). More importantly, we show in Supp. Table S4 that the K isotopic offset between seawater and a number of USGS standards is virtually indistinguishable across labs, attesting to the efficacy of existing methods for high-precision K isotopic ratio analyses.

The external reproducibility of our protocols (chromatography and mass spectrometry) was determined through replicate measurements of international standards. Isotopic compositions of all measured standards are indistinguishable from published values: $\delta^{41}K_{Seawater}$= -0.02 ±0.17‰ (2σ, n=30; Morgan et al., 2018), $\delta^{26}Mg_{Cambridge}$= -2.57 ±0.08‰ (2$\sigma$, n=8; Galy et al., 2003), $\delta^{7}Li_{L-SVEC}$= 0.01 ±0.80‰ (2σ, n=21; Millot et al., 2004), and $^{87}Sr/^{86}Sr_{BCR-2}$= 0.705032 ±40 (2$\sigma \times 10^{-6}$, n=13; Weis et al., 2006). For samples analyzed once (chromatography and mass spectrometry), reported errors are the 2σ uncertainties of the external standard for that isotopic system. In cases where samples were analyzed multiple times, reported errors are twice the standard error of the mean (2SE). Replicate analyses improved uncertainties in measurements of Li, K, and Sr isotopes. In the case of Mg, 67% of replicated analyses (28 of 42) yielded uncertainties smaller than or equal to this laboratory's long-term external precision of 0.09‰ (Supp. Table S1).

4. Results

Ti-normalized elemental ratios, isotopic measurements, and XRD mineral abundances are listed in Supplementary Tables S1–S3 and shown in Figs. 2–6.

4.1. The composition of AOC from Troodos ophiolite and ODP Hole 801C

4.1.1. K/Ti and Mg/Ti ratios

Whole-rock samples from the Troodos ophiolite span a large range of K/Ti ratios with 79% being elevated compared to unaltered basalt (Supp. Table S1; Fig. 2A, C). The average K/Ti ratio of the sample suite is ~12x higher than unaltered Troodos glass (K/Ti= 0.40 ±0.18, 1σ, n=184; Regelous et al., 2014; Coogan and Gillis, 2018). Seven samples from Klirou, near the lava-dike boundary, show either no K enrichment or a lower K/Ti ratio compared to unaltered glass. Whole-rock samples from Hole 801C all have higher K/Ti ratios than fresh basalt (K/Ti= 0.01 to 0.11; Fisk and Kelley, 2002; Alt and Teagle, 2003), with an average of 0.50 ±0.33 g/g (1σ, n=17). Three celadonite mineral separates from Troodos have much higher K/Ti ratios than any whole-rock sample in the ophiolite (avg. K/Ti= 442 ±153 g/g, 1σ). Sampled veins from Hole 801C also show elevated K/Ti ratios of 1.39 to 47.61 g/g, or 10 to 1000x higher than the unaltered basalt.

Measured Mg/Ti ratios (Supp. Table S1) mostly fall within the observed range of unaltered glass for both Troodos (1.11 to 16.75 g/g) and Hole 801C (1.94 to 6.11 g/g). There are a few exceptions at both sites, with values that are lower and higher than reported glass compositions (Fig. 2B). As in the case for K/Ti ratios, the celadonite separates from Troodos are characterized by elevated Mg/Ti ratios (229 ±73 g/g, 1σ). At Hole 801C, three out of six sampled veins are enriched in Mg/Ti compared to unaltered compositions, with ratios up to 63.11 g/g.

4.1.2. Radiogenic Sr

Supplementary Table S1 contains measured $^{87}Sr/^{86}Sr$ ratios for Troodos and Hole 801C samples as well as ratios corrected for radiogenic ingrowth from Rb decay, assuming crustal formation ages of 91.6 Ma (Troodos) and 167 Ma (Hole 801C). Age-corrected $^{87}Sr/^{86}Sr$ ratios (Fig. 2A) from the Troodos ophiolite (0.70365 – 0.70837) and Hole 801C (0.70303 – 0.70853) are variably more radiogenic than the unaltered end-members (0.7035 and 0.7024, respectively; Rautenschlein, 1987; Hauff et al., 2003), and positively correlate with K/Ti ratios. Troodos samples with $^{87}Sr/^{86}Sr$ ratios similar to unaltered basalt (0.70365 – 0.70383) are from basal group site Klirou. $^{87}Sr/^{86}Sr$ ratios in Troodos samples span the entire range from pristine basalt to 71-91 Ma seawater, with 12 samples having $^{87}Sr/^{86}Sr$ ratios that are more radiogenic than late Cretaceous seawater. Age-corrected $^{87}Sr/^{86}Sr$ ratios from Hole 801C are mostly lower than Jurassic seawater, with one exception. In both Troodos and Hole 801C, the most radiogenic samples have Rb/Sr ratios on the higher end of the range of measured values (Supp. Table S1), suggesting that Rb loss may, in part, explain $^{87}Sr/^{86}Sr$ values that are more radiogenic than coeval seawater.

4.1.3. Mg isotopes

Measured $\delta^{26}Mg$ values for 90 bulk-rock samples and 3 mineral separates from the Troodos ophiolite range from -0.73‰ to +0.50‰. Only four samples have $\delta^{26}Mg$ values lower than MORB ($\delta^{26}Mg$= -0.25 ±0.04‰; Teng, 2017); two of these are celadonite mineral separates (both have $\delta^{26}Mg$= -0.59‰) and one ($\delta^{26}Mg$= -0.73‰) is the deepest sample from core CY1a, at ~460 m below the sediment-basement interface (Fig. 2B). In contrast, 88 of the 90 whole-rock samples from Troodos have $\delta^{26}Mg$ values higher than MORB, even though Mg/Ti ratios are mostly indistinguishable from glass values. The average $\delta^{26}Mg$ of bulk-rock samples from Troodos (weighted by Mg/Ti; Fig. 3B, Supp. Info. F) is +0.01 ±0.02‰ (1σ, n=90). Measured $\delta^{26}Mg$ values for 23 bulk-rock and vein samples at Hole 801C range from -0.11‰ to +0.92‰ (Fig. 2B), with weighted average of +0.21 ±0.06‰ (1σ, n=17; Supp. Info. F); all 801C samples have $\delta^{26}Mg$ values similar to or higher than MORB and no correlation is observed between $\delta^{26}Mg$ and Mg/Ti. Our results are similar to the range of $\delta^{26}Mg$ values, -1.70‰ to +0.21‰ (n=15), recently published by Huang et al. (2018) on individual samples from a similar crustal depth interval at Hole 801C.

4.1.4. K isotopes

Potassium isotopic compositions of bulk rock and mineral separates from the Troodos ophiolite and ODP Hole 801C range from -1.07‰ to +0.01‰ (n = 83) and -0.88‰ to +0.04‰ (n = 17), respectively (Fig. 2C). The variability in $\delta^{41}K$ values at both sites is ~1‰ and spans values that are both lower and higher than BSE ($\delta^{41}K$= -0.54 ±0.17‰; e.g. Morgan et al., 2018). The lowest $\delta^{41}K$ value measured at Troodos is a celadonite mineral separate from Onophrious (2014CL 200A). Mineral separates from Troodos and veins from 801C have higher K/Ti than bulk-rock samples and show lower average $\delta^{41}K$ values: -0.88 ±0.17‰ (1σ) for Troodos celadonites (n=3) and -0.58 ±0.21‰ (1σ) for Hole 801C veins (n=5). Excluding the celadonites, the range of $\delta^{41}K$ compositions from Troodos rocks (-0.97‰ to 0.01‰) is similar to that of Hole 801C (-0.88‰ to 0.04‰), and at both locales measured $\delta^{41}K$ values do not strongly correlate with K/Ti ratios (Fig. 2C). When weighted by K/Ti ratios (Supp. Info. F), whole-rock samples from the Troodos ophiolite yield an average $\delta^{41}K$ value of -0.48 ±0.20‰ (1σ, n=80; Fig. 3A), indistinguishable from the weighted average for whole-rock samples from Hole 801C (-0.49 ±0.18‰, 1σ, n=12), and BSE (-0.54 ±0.17‰). The highest $\delta^{41}K$ values from Troodos are from Klirou, with two of six samples characterized by $\delta^{41}K$ compositions that are similar to modern seawater. The two samples from Hole 801C with the heaviest $\delta^{41}K$ values (-0.20‰ and 0.04‰) come from shallow crustal depths (156-167 meters) and are associated with the least radiogenic $^{87}Sr/^{86}Sr$ ratios measured at that site.

4.2. Troodos ophiolite mineralogy

The composition of secondary minerals in altered oceanic crust has been argued to control, at least in part, the net isotopic frac-

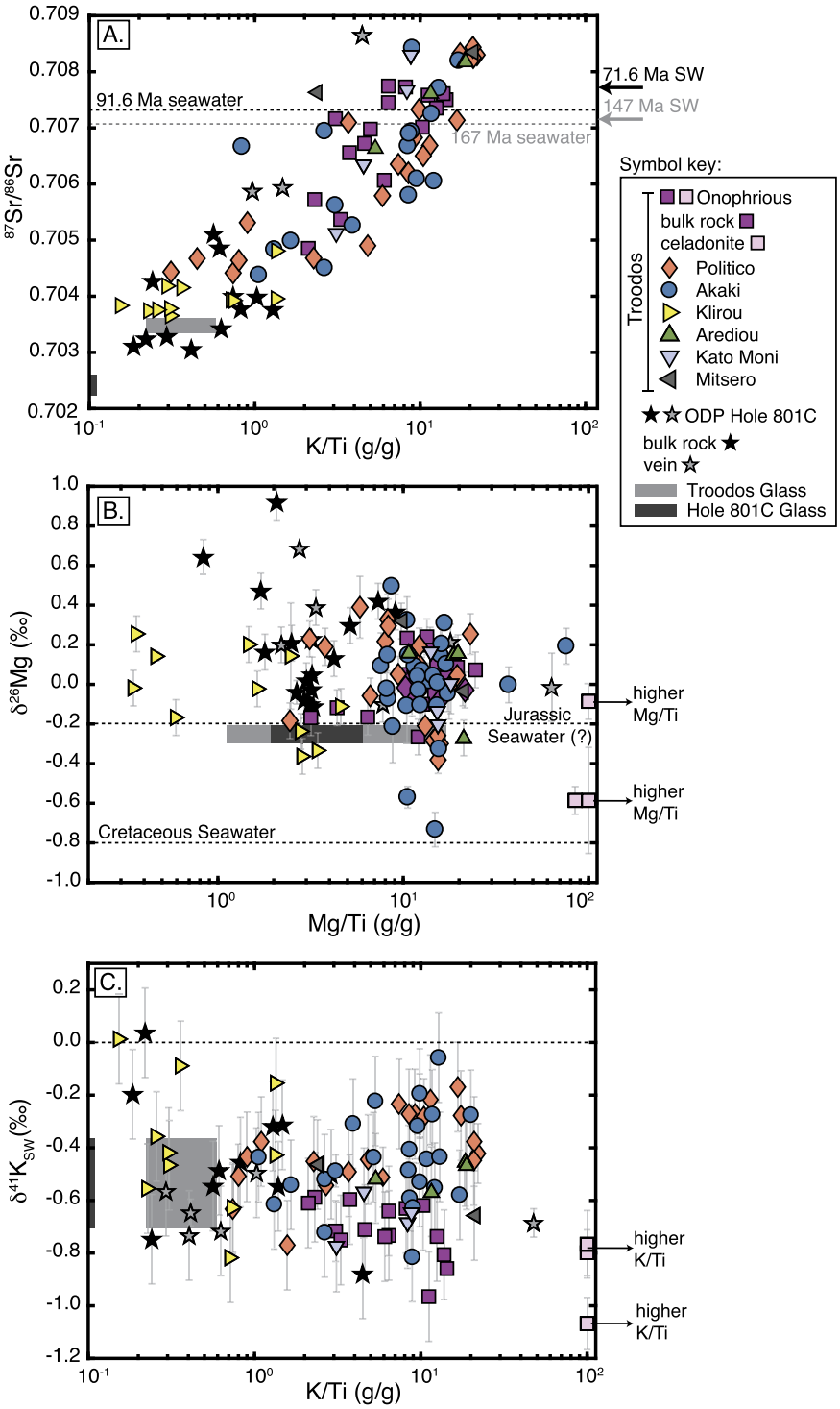

Fig. 2. Elemental and isotopic compositions of Troodos ophiolite and Hole 801C. (A) Age-corrected $^{87}Sr/^{86}Sr$ ratios for Troodos ophiolite (91.6 Ma) and Hole 801C (167 Ma) show a strong correlation with K/Ti ratio, suggesting extensive basalt-seawater exchange and crustal uptake of seawater-K; (B) $\delta^{26}Mg$ values of AOC from both Troodos and Hole 801C are mostly elevated compared to unaltered basalt, even when Mg/Ti ratios remain virtually unchanged; (C) AOC samples from both sites show a large range in $\delta^{41}K$ compositions, with values that are both heavier and lighter than bulk silicate Earth (BSE). (A–C) Shaded boxes represent the elemental and isotopic compositions of the unaltered glass end-members for both Troodos (light gray) and Hole 801C (dark gray), while dashed lines represent compositions for Jurassic/Cretaceous seawater (see text for details). Errors on the isotopic composition of unaltered glass are 0.04‰ for $\delta^{26}Mg$ (Teng, 2017) and 0.17‰ for $\delta^{41}K$ (Morgan et al., 2018). Since errors on $^{87}Sr/^{86}Sr$ ratios are too small at this scale, the thickness of the shaded areas in panel (A) was arbitrarily set to equal the size of data symbols.

tionation between fluid and altered basalts (e.g. Coogan et al., 2017). To test the hypothesis that the observed range in $\delta^{41}K$ compositions of Troodos ophiolite samples might be explained by variable secondary mineralogy, we analyzed the mineral makeup of a subset of samples from Onophrious (n=14), Politico (n=24), and Akaki (n=4). We chose to focus on these Troodos sites because of the well-documented differences in alteration styles and the potential for systematic differences in secondary mineralogy (Coogan et al., 2017; Gillis et al., 2015).

Primary mineralogy of the Onophrious, Politico and Akaki samples analyzed here is composed of plagioclase (0-57 wt%, n=39), clinopyroxene (1-19 wt%, n=38), and magnetite (0-2 wt%, n=42),

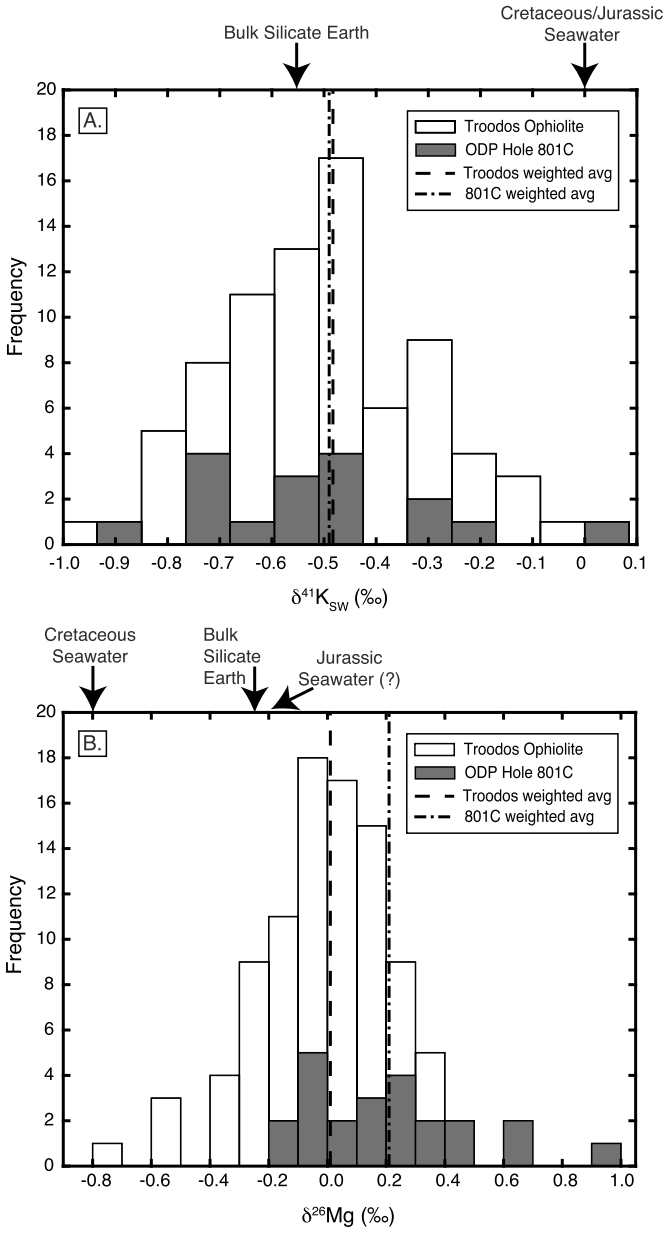

Fig. 3. Comparison of bulk δ^{41}K, δ^{26}Mg compositions of AOC from the Troodos ophiolite and Hole 801C. Histograms show distributions of δ^{41}K (A) and δ^{26}Mg (B) compositions, while dashed lines represent the average δ^{41}K (A) and δ^{26}Mg (B) values for both sites weighted by their K/Ti and Mg/Ti ratios, respectively. Arrows mark the δ^{41}K and δ^{26}Mg compositions of ancient seawater (see text for details) and bulk silicate Earth (Teng, 2017; Morgan et al., 2018) for reference.

with fewer occurrences of amphibole (0-6 wt%, n=8) and ilmenite (<0.3 wt%, n=6) (Supp. Table S3). Alteration mineralogy mainly consists of mixtures of trioctahedral smectite (12-72 wt%, n=42), K-feldspar (1-41 wt%, n=42), calcite (0-32 wt%, n=39), dioctahedral mica (0-18 wt%, n=36), and chlorite (0-2 wt%, n=39) (Supp. Tables S2-S3). Goethite, an iron-oxyhydroxide phase, is absent from Onophrious, but ranges up to 2 wt% (n=21) at Politico/Akaki (Supp. Tables S2-S3). Although celadonite is a common dioctahedral mica in AOC, little to no celadonite was detected in these samples. With the exception of chlorite, the minerals observed at Troodos are typical of low-temperature alteration of oceanic crust (Gillis and Robinson, 1991). Among the secondary phases identified here, the main potential K-bearing minerals are K-feldspar, dioctahedral mica, and, to a lesser extent, smectite. In addition, a strong positive correlation is observed between K_2O and K-feldspar wt% at all sites (R^2 = 0.90; Fig. 6A), indicating that this mineral is the major sink of seawater K in the samples analyzed here. In addition to K, smectites are also potential hosts for Mg and Li in these altered basalts (e.g. Gillis et al., 2015).

5. Discussion

The low-temperature alteration of oceanic crust by seawater removes K, Mg, and Li from the ocean at rates that are potentially of the same order of magnitude as the fluxes of these elements in rivers draining the continents (Hart and Staudigel, 1982; Elderfield and Schultz, 1996). As such, understanding low-temperature oceanic crust alteration will contribute invaluable information on the mechanisms controlling seawater chemistry in the modern and through time. This study presents the first dataset with paired K, Mg, and Li isotopes in AOC from the Troodos ophiolite (91.6 Ma) and ODP Hole 801C (167 Ma) in an effort to (1) quantify K isotope fractionation during low-temperature alteration of oceanic crust and estimate its role in elevating the ^{41}K/^{39}K of seawater compared to BSE and (2) pair these measurements with analyses of δ^{26}Mg and δ^{7}Li values to develop an isotopic fingerprint for the alteration of oceanic crust at low temperatures.

5.1. Potassium isotope mass balance during low-temperature oceanic crust alteration

Both Troodos and Hole 801C show clear evidence of extensive reaction with seawater for a few tens of millions of years after crust formation from age-corrected ^{87}Sr/^{86}Sr ratios (e.g. Hart and Staudigel, 1982; Alt and Teagle, 1999). K uptake during low-temperature alteration of oceanic crust has been previously reported for both Troodos ophiolite and Hole 801C samples (Bednarz and Schmincke, 1989; Plank et al., 2000) and is corroborated here by the strong positive correlation between K/Ti and ^{87}Sr/^{86}Sr ratios in both sites (Fig. 2A). As most seawater-K uptake occurs in the upper volcanics (e.g. Bednarz and Schmincke, 1989), it is not surprising that the few Troodos samples (n=5) with K contents and ^{87}Sr/^{86}Sr ratios similar to the unaltered glass are all from basal volcanics at Klirou.

Although we do not know the δ^{41}K value of seawater at the time of low-temperature alteration of the Troodos ophiolite or Hole 801C, two lines of evidence suggest that its δ^{41}K value was within ~0.2‰ of the modern seawater composition. First, δ^{41}K values in bulk samples that approach modern seawater at both Troodos and Hole 801C are difficult to explain if the δ^{41}K of seawater was significantly lower than modern. Elevation of bulk-rock δ^{41}K values due to Rayleigh-type distillation of the hydrothermal fluid is unlikely as (1) the fraction of seawater K removed during low-temperature alteration is generally small (i.e. <5%; e.g. Wheat and Fisher, 2008) and (2) a lower δ^{41}K of seawater would mean less K isotope fractionation between seawater and AOC at both sites, making it more difficult to elevate fluid δ^{41}K values with isotopic distillation. Second, a recent study by Li et al. (2019) found that while the formation of secondary clays during continental silicate weathering preferentially retains ^{39}K, the magnitude of this effect is relatively small, e.g. an order of magnitude change in weathering intensity is expected to change the δ^{41}K of the river flux by only ~0.2‰. Taken together, these observations suggest that the δ^{41}K of seawater in the Jurassic and Cretaceous was likely close to the modern value (δ^{41}K ~0‰). Considered in this light, the observation that δ^{41}K values for both the Troodos ophiolite and ODP Hole 801C are ~0.5‰ lower than modern seawater implies that the low-temperature alteration of oceanic crust preferentially removes ^{39}K from seawater. Assuming Cretaceous/Jurassic seawater with a δ^{41}K value indistinguishable from the modern yields a fractionation factor ($\alpha_{solid-fluid}$) for ^{41}K/^{39}K of ~0.9995, similar in

both magnitude and direction to estimates of K isotope fractionation associated with the formation of authigenic silicates during marine sediment diagenesis (Santiago Ramos et al., 2018) and continental weathering (Li et al., 2019).

The large range in δ^{41}K values reported here contrasts with results from Parendo et al. (2017), who concluded, based on 6 analyses of altered basalts/gabbros from the Bay of Islands Ophiolite, that K isotopes were not fractionated during low-temperature basalt alteration. The apparent discrepancy between the two studies is likely related to the absence of samples from the upper volcanics in the ophiolite studied by Parendo et al. (2017). Samples analyzed in that study originate from deeper within the ophiolite sequence (>400 m), where conditions of alteration are distinct from those of the upper volcanic sequence. For example, the lower water-to-rock ratios and higher alteration temperatures in the sheeted dikes and gabbros may lead to K being leached from the crust rather than added to the crust at depth. Additionally, the secondary minerals formed at these temperatures are distinct from low-temperature assemblages (e.g. Gillis and Robinson, 1991). Finally, the observed K/Ti ratios of the volcanic samples studied by Parendo et al. (2017) are much lower (0.23 to 0.66 g/g, n=3) than those in the upper volcanics analyzed at both Troodos and Hole 801C, and may not accurately reflect the average isotopic composition of the seawater K sink in altered oceanic crust.

5.2. Magnesium isotope mass balance during low-temperature oceanic crust alteration

Compared to K, the Mg sink in low-temperature AOC is more difficult to quantify due to the high initial Mg content of unaltered oceanic crust, sources of variability unrelated to low-temperature alteration (e.g. fractional crystallization), and sampling biases associated with incomplete recovery of drilled oceanic crust (e.g. Coogan and Gillis, 2018). Mg isotopes have emerged as a potentially powerful tool for constraining Mg fluxes between seawater and AOC, as the incorporation of Mg into secondary clays fractionates Mg isotopes; studies in both laboratory and natural settings indicate that secondary clays are characterized by δ^{26}Mg values that are up to 1.25‰ higher than the fluid (Wimpenny et al., 2014; Dunlea et al., 2017). As a result, depending on the δ^{26}Mg value of seawater, the secondary clays in low-temperature AOC may be either heavier or lighter than the δ^{26}Mg value of unaltered oceanic crust.

Results from both the Troodos ophiolite and ODP Hole 801C indicate that low-temperature AOC is associated with an increase in bulk-rock δ^{26}Mg compositions; average δ^{26}Mg values, weighted by Mg/Ti ratios, are +0.01 $\pm$0.02‰ (1σ) and +0.21 $\pm$0.06‰ (1σ) for samples from Troodos and Hole 801C, respectively. These values are ~0.2 to 0.4‰ higher than the MORB δ^{26}Mg composition and indicate that low-temperature alteration of oceanic crust is a sink of ^{26}Mg from seawater. The average δ^{26}Mg composition presented here for Hole 801C is similar to, but higher than, the δ^{26}Mg value of 0.00 $\pm$0.09‰ (2σ, n=12) observed by Huang et al. (2018), a difference likely due to the limited size of both datasets. When light (n=2) and heavy (n=3) δ^{26}Mg outliers are excluded, both datasets are characterized by a similar range in ^{26}Mg values: -0.11‰ to +0.47‰ (this study) and -0.35‰ and +0.21‰ (Huang et al., 2018).

The observation that, at both Troodos and Hole 801C, low-temperature oceanic crust alteration leads to an increase in bulk-rock δ^{26}Mg values, despite the fact that seawater has a much lower δ^{26}Mg value than unaltered oceanic crust, is consistent with the preferential incorporation of ^{26}Mg in secondary clays formed during basalt-seawater exchange. Reconstructions of the δ^{26}Mg of seawater since the Mesozoic from fossil corals indicate that the δ^{26}Mg of seawater at the time of alteration of the Troodos ophiolite was within a few tenths of a permil of modern seawater (~-0.80‰; Gothmann et al., 2017). Taking the difference between this seawater δ^{26}Mg value and the highest measured δ^{26}Mg value at Troodos, we estimate that the magnitude of Mg isotope fractionation associated with the Mg sink in low-temperature AOC is at least ~1.30‰, a value that is indistinguishable from available estimates of Mg isotope fractionation during secondary clay formation (Wimpenny et al., 2014; Dunlea et al., 2017). Despite the lack of definitive archives of seawater δ^{26}Mg values coincident with the time of low-temperature alteration at Hole 801C, upper Triassic shallow-water dolomites (Geske et al., 2012) are characterized by δ^{26}Mg values that are 0.6 to 0.8‰ higher than Neogene shallow-water dolomites (Fantle and Higgins, 2014; Higgins et al., 2018). Although we cannot exclude local fluid evolution and variable formation temperatures may explain, in part, the difference in δ^{26}Mg values between Triassic and Neogene dolomites, a δ^{26}Mg value of seawater of ~-0.2‰ in the Triassic is the most straightforward explanation. Accordingly, we note that the highest measured δ^{26}Mg value from bulk-rock samples at Hole 801C is 0.92‰, or ~1.12‰ higher than Triassic-Jurassic seawater, again, similar to estimates of Mg isotope fractionation associated with secondary clay formation (Wimpenny et al., 2014; Dunlea et al., 2017).

Although our results for Hole 801C do not capture the low δ^{26}Mg values observed in Huang et al. (2018), two bulk-rock samples from the Troodos ophiolite (CY1a-14.96 and CY1-298.3) have δ^{26}Mg compositions (-0.73‰ and -0.57‰, respectively) that are lighter than MORB (δ^{26}Mg = -0.25 $\pm$0.04‰; Teng, 2017). Potential explanations for δ^{26}Mg values lower than unaltered basalt include exchange with evolved fluids, which become enriched in ^{24}Mg due to the formation of secondary silicates, and higher carbonate contents, as carbonates tend to be characterized by δ^{26}Mg values that can be >3-4‰ lower than unaltered basalt (Higgins and Schrag, 2010; Huang et al., 2018). For sample CY1a-14.96, its small carbonate content, along with the low abundance of Mg in calcite, suggest that the presence of carbonates cannot explain the sample's low δ^{26}Mg value. As this is the deepest sample in the Akaki site (~460 m), Rayleigh-type distillation of the alteration fluid due to formation of secondary clays is the more likely explanation for the light δ^{26}Mg composition observed. In contrast, the high Ca content of sample CY1-298.3 (~20 wt% CaO; Coogan et al., 2017) suggests this sample contains substantial calcite (~15-25%) that is probably sufficient to explain its light δ^{26}Mg value, assuming a low-Mg calcite end-member with δ^{26}Mg of ~-4.25‰. Finally, carbonates cannot account for the low δ^{26}Mg in two celadonite separates. Although Rayleigh distillation is a plausible explanation for the light Mg-isotopic composition of these celadonites, another possibility is that the celadonite structure fractionates Mg isotopes differently than most clays.

5.3. Decoupling of elemental and isotopic fluxes of Mg during oceanic crust alteration at low temperatures (<100 °C)

Measured Mg/Ti ratios for almost all of the bulk samples from the Troodos ophiolite and ODP Hole 801C fall within the range of protolith compositions at both sites (Fig. 2B). However, in spite of the lack of variability in bulk-rock Mg/Ti ratios, most of our AOC samples are characterized by Mg-isotopic compositions that are elevated (δ^{26}Mg up to 0.92‰) compared to unaltered MORB (δ^{26}Mg= -0.25 $\pm$0.04‰; Teng, 2017). The highest measured δ^{26}Mg values in bulk samples from Troodos and 801C, reflecting the most isotopically modified samples, are ~1.12 to 1.30‰ higher than seawater. This isotopic difference is similar to the fractionation factor for clay minerals formed at low-temperatures (Dunlea et al., 2017; Wimpenny et al., 2014), suggesting that the Mg in these samples has undergone virtually complete isotopic exchange with seawater Mg despite little change in the bulk Mg content. The mechanism for this exchange is likely the concurrent dissolution of Mg-bearing

primary phases and growth of secondary Mg-clays such as smectite. This isotopic effect is similar to what has been previously described for $^{87}Sr/^{86}Sr$ isotopes during low-temperature basalt alteration of the upper volcanics (e.g. Butterfield et al., 2001).

The recognition that chemical and isotopic fluxes of Mg are decoupled during the low-temperature alteration of basalt has important consequences for the Mg isotopic budget of seawater. In particular, it indicates that low-temperature oceanic crust alteration could play an important role in determining the δ^{26}Mg value of seawater even if the net sink of seawater Mg in oceanic crust is small. Using the Troodos ophiolite as an example, if we assume a δ^{26}Mg value of seawater of -0.8‰, a fractionation factor associated with Mg removal during low-temperature oceanic crust alteration of 1.3‰, and an average δ^{26}Mg value of AOC of ~0‰ (weighted by Mg/Ti ratio), we estimate that ~33% of the Mg in the bulk crust was isotopically exchanged with seawater. Averaged over 300-600 meters of altered oceanic crust and assuming a protolith MgO content of 6.8 wt%, we estimate a gross exchange flux between seawater and crust of 1.4 to 2.7 Tmol of Mg/yr, or 27% to 54% of the modern riverine Mg flux.

5.4. Site-to-site variability in the $\delta^{41}K$ and $\delta^{7}Li$ of low-temperature AOC in the Troodos ophiolite

Our results show large and, in some cases, systematic ranges in the isotopic ratios of $^{7}Li/^{6}Li$ (~7‰), $^{26}Mg/^{24}Mg$ (>1.20‰) and $^{41}K/^{39}K$ (~1‰) across the Troodos ophiolite. In particular, histograms of δ^{41}K and δ^{7}Li values for the three sites of upper volcanic rocks indicate that Onophrious is distinct for both δ^{41}K and δ^{7}Li values (Fig. 4). While δ^{41}K values in Politico and Akaki span a similar range (-0.77‰ to -0.17‰ and -0.81‰ to -0.06‰, respectively), Onophrious samples show a much lighter isotopic distribution (-0.97‰ to -0.59‰; Fig. 4A). When celadonite mineral separates are included, the lowest δ^{41}K value at Onophrious reaches -1.07‰. A similar pattern is observed in δ^{7}Li values (Fig. 4B); Politico and Akaki yield similar distributions and a combined range of δ^{7}Li values between 6.71‰ and 12.6‰. In contrast, measured δ^{7}Li values from bulk-rock samples at Onophrious are lower, ranging from 6.29‰ to 9.10‰. Celadonite mineral separates from the same locale are characterized by even lighter δ^{7}Li values (5.80‰ to 7.27‰; Coogan et al., 2017). In addition to the differences in δ^{41}K and δ^{7}Li values, Onophrious is also characterized by smaller K and Li enrichments and the absence of Fe-oxyhydroxides (Supp. Table S1–S2; Coogan et al., 2017). In the following section we evaluate the potential sources of this variability, including (1) Rayleigh distillation of the aquifer fluid, (2) temperature of the aquifer fluid, (3) mineralogy, and (4) the relative importance of advective and diffusive supply of K and Li and its effect on net isotopic fractionation during low-temperature oceanic crust alteration.

5.4.1. Rayleigh distillation of the aquifer fluid

Sediment cover inhibits fluid ingress into the oceanic crust and leads to fluid recharge being focused on unsedimented regions. As a result, fluids feeding sedimented areas have to be transported there by lateral flow in the aquifer, leading to a more evolved fluid composition due to fluid-rock reactions along the flow path (e.g. Farahat et al., 2017; Lauer et al., 2018). Thus, we expect higher water-to-rock ratios, and an aquifer fluid composition less shifted from seawater, in the Akaki/Politico areas compared to Onophrious, which was sedimented much earlier. In fact, the absence of Fe-oxyhydroxides in our Onophrious samples is consistent with the presence of evolved fluids with low oxidizing power (e.g. Kuhn et al., 2017).

During fluid-rock reactions, the precipitation of secondary K,Li-silicates, which are enriched in the light isotope (^{6}Li, ^{39}K), is expected to drive δ^{7}Li, δ^{41}K values higher in fluids that have reacted with more rock. However, this behavior is precisely the opposite of what is observed in the Troodos ophiolite, as samples from Onophrious are characterized by systematically lower δ^{7}Li and δ^{41}K values compared to Akaki/Politico. In addition, though K_2O (up to 4.80 wt%; Supp. Table S2) and Li (up to 73 ppm; Gillis et al., 2015; Coogan et al., 2017) contents observed at Onophrious are lower than Akaki/Politico, they still imply water-to-rock ratios of 100' to 1000's g/g. Under these conditions, secondary mineral formation is unlikely to substantially modify the isotopic composition of the fluid, further indicating that Rayleigh distillation of K and/or Li in the aquifer fluid cannot explain the overall lower δ^{41}K and δ^{7}Li values observed at Onophrious relative to Akaki/Politico.

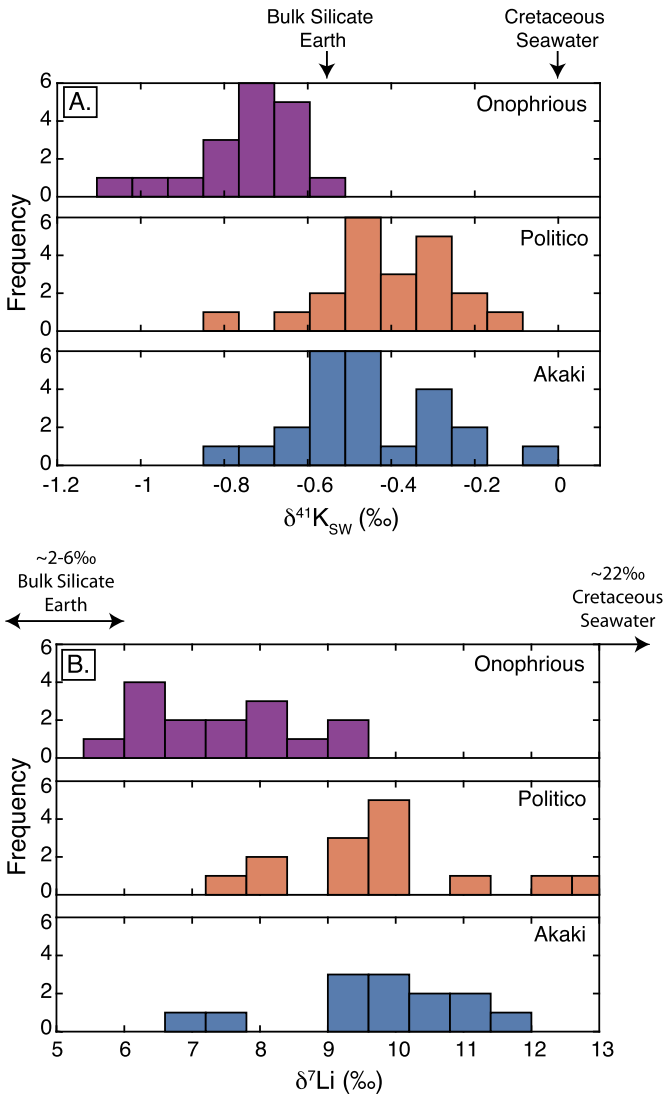

Fig. 4. Site-to-site variability in δ^{41}K and δ^{7}Li compositions across the Troodos ophiolite. Distributions of δ^{41}K (A) and δ^{7}Li (B) values for Onophrious, Politico and Akaki show the distinct isotopic composition of the Onophrious site in both isotope systems. Bulk silicate Earth (e.g. Tomascak et al., 2008; Morgan et al., 2018) and Cretaceous seawater compositions are indicated for reference. See text for details on how we estimate the δ^{41}K composition of Cretaceous seawater; for the δ^{7}Li value of Cretaceous seawater, we use that of Pogge Von Strandmann et al. (2013).

5.4.2. Temperature of the aquifer fluid

Differences in fluid temperatures between Onophrious and Akaki/Politico are unlikely to be sufficient to explain their distinct δ^{41}K and δ^{7}Li distributions. Based on the δ^{18}O values of secondary calcite amygdales, Coogan et al. (2019) have shown that, over the

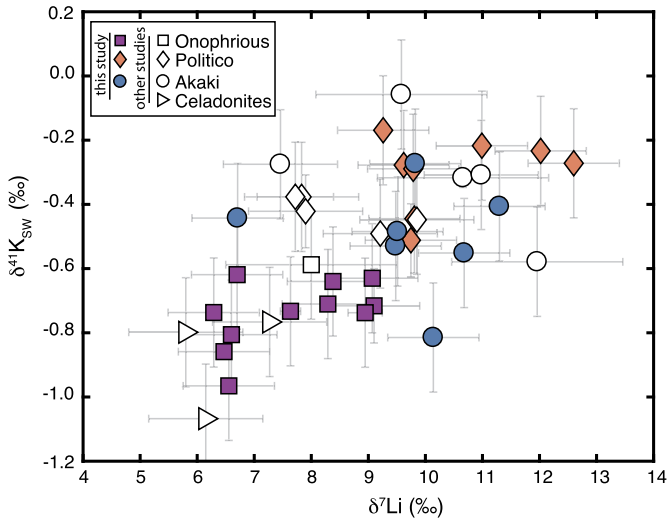

Fig. 5. Cross-plot of δ^{41}K (y-axis) and δ^{7}Li (x-axis) values in Troodos sites. Correlation between δ^{41}K and δ^{7}Li likely results from the combined effects of variable mineralogy and diffusive exchange between the crust and overlying sedimentary pore-fluid, as both K and Li isotopes fractionate during diffusion (e.g. Richter et al., 2006; Bourg et al., 2010). Closed symbols represent δ^{7}Li data from this study, while open symbols correspond to δ^{7}Li values from Gillis et al. (2015) and Coogan et al. (2017).

depth range where most of our samples come from, alteration temperatures at Onophrious are indistinguishable from those at Politico and Akaki and similar to coeval seawater. This suggests that all three sites experienced comparably low temperatures during the period of alteration that coincides with the formation of calcite. In addition, the δ^{41}K and δ^{7}Li values at Onophrious are lower than those at Akaki and Politico, whereas if early sedimentation led to elevated temperatures at Onophrious, this should lead to smaller fractionation of K and Li isotopes, and thus heavier δ^{41}K and δ^{7}Li compositions.

5.4.3. Mineralogy

Another possible explanation for the systematic differences in δ^{41}K and δ^{7}Li values between Onophrious and Politico/Akaki is variable secondary mineralogy. K isotope fractionation during marine silicate diagenesis was speculated to be dependent on the coordination number of potassium in the secondary silicate product (Santiago Ramos et al., 2018). Crystal bonding environment also appears to control the δ^{7}Li of silicates, as has been demonstrated for Li-clays synthesized in the laboratory (Hindshaw et al., 2019). Finally, differences in the mineralogy and abundance of alteration products have been proposed to explain the large range in Li isotopic composition of altered basalts from Troodos, including a number of the samples discussed here (Coogan et al., 2017). In fact, the correlation we observe between δ^{41}K and δ^{7}Li values within our Troodos samples (Fig. 5) could be related to variations in mineral-specific fractionations, given that some alteration products host both cations (e.g. celadonite).

XRD results for 42 Troodos samples indicate that their overall K_2O content is largely controlled by secondary K-feldspar abundance; K-feldspar and K_2O wt% strongly correlate in these samples and the slope of the relationship is indistinguishable from that expected for an "ideal" K-feldspar (17 wt% K_2O; Fig. 6A). For samples that are more K-enriched than predicted from K-feldspar abundances, other K-bearing minerals must be present (e.g. celadonite) and could affect the overall δ^{41}K, δ^{7}Li compositions of the bulk sample. Although all three celadonite separates measured here from Onophrious indeed have δ^{41}K (-1.07‰ to -0.77‰) and δ^{7}Li (5.80‰ to 7.27‰; Coogan et al., 2017) values lower than the average Troodos crust, celadonite was not detected in any of the bulk samples analyzed for mineralogy. Even if all the dioctahedral mica were prescribed to celadonite, its abundance is considerably smaller than K-feldspar, and there are no major differences in the mica content of the samples studied here from Onophrious relative to Akaki/Politico (Supp. Table S2). Further, Fig. 6B clearly shows samples with similarly high K-feldspar content and very different δ^{41}K values, indicating that mineralogy is unlikely to be the main source of the systematically lower δ^{41}K and δ^{7}Li values observed at Onophrious.

5.4.4. Advective vs. diffusive supply of cations

The recognition that most site-to-site variability in δ^{41}K and δ^{7}Li values between Onophrious and Akaki/Politico cannot be fully explained by differences in fluid chemistry, temperature or secondary mineralogy implies the existence of alternative sources of local isotopic variability. One intriguing possibility is that the low δ^{41}K and δ^{7}Li values at Onophrious reflect a greater role for the diffusive supply of these cations at this site. As sediment thickness increases, the mode of cation transport through the sediment column to the underlying crust changes from advection to diffusion (McDuff, 1981; Elderfield et al., 1999; Wheat and Mottl, 2000; Mewes et al., 2016). Recent work on the K cycling in deep-sea sediments has shown that the δ^{41}K composition of marine pore-fluids is affected by diffusive K fractionation, as ^{39}K diffuses through the sediment pore-fluid at a faster rate than ^{41}K (Bourg et al., 2010; Santiago Ramos et al., 2018). With measured pore-fluid δ^{41}K values as low as -2‰ (Santiago Ramos et al., 2018), local K supply from diffusion could affect the overall δ^{41}K of aquifer fluids even though the amount of K supplied by diffusion would remain small relative to K supplied by hydrothermally advected fluids. In addition, as Li isotopes also fractionate during aqueous diffusion (Richter et al., 2006; Bourg et al., 2010), diffusive fractionation of both K and Li isotopes provides a plausible mechanism for both the low δ^{7}Li values at Onophrious and the positive correlation between δ^{41}K and δ^{7}Li values in our samples from the Troodos ophiolite (Fig. 4-5).

6. Conclusions

The seawater δ^{41}K value is elevated by ~0.5‰ relative to bulk silicate Earth for reasons that remained enigmatic until recently. Here, we presented δ^{41}K measurements from a large sample suite of bulk-rock, veins, and mineral separates from AOC in the Troodos ophiolite and ODP Hole 801C; our results indicate that the elevated δ^{41}K value of seawater can be explained, in part, by the preferential incorporation of ^{39}K into secondary silicates formed during the low-temperature alteration of oceanic crust by seawater. Average K isotope fractionation factors estimated for the K sink in AOC are ~-0.5‰, and the weighted average K sink in AOC for both Troodos and Hole 801C are indistinguishable from each other and from BSE; however, both sites show significant variability in δ^{41}K compositions, with values that are both higher and lower than BSE.

Our reported fractionation factors for Mg incorporation into AOC from Troodos (~+1.3‰) and Hole 801C (~+1.1‰) are similar to previous estimates of Mg isotope effects associated with secondary clay formation in both laboratory (Wimpenny et al., 2014) and natural settings (Dunlea et al., 2017). Our results thus confirm that secondary silicate formation in AOC is a sink of ^{26}Mg from seawater, in line with recent findings by Huang et al. (2018) and Shalev et al. (2019). Together, these results indicate that the AOC Mg sink explains, in part, the light δ^{26}Mg composition of seawater (~-0.8‰). In addition, our results point to a decoupling of elemental and isotopic fluxes of Mg during basalt alteration by seawater, suggesting that Mg isotope exchange during low-temperature oceanic crust alteration may play an outsized role in the Mg isotopic budget of seawater even if the net fluxes of Mg into AOC are small.

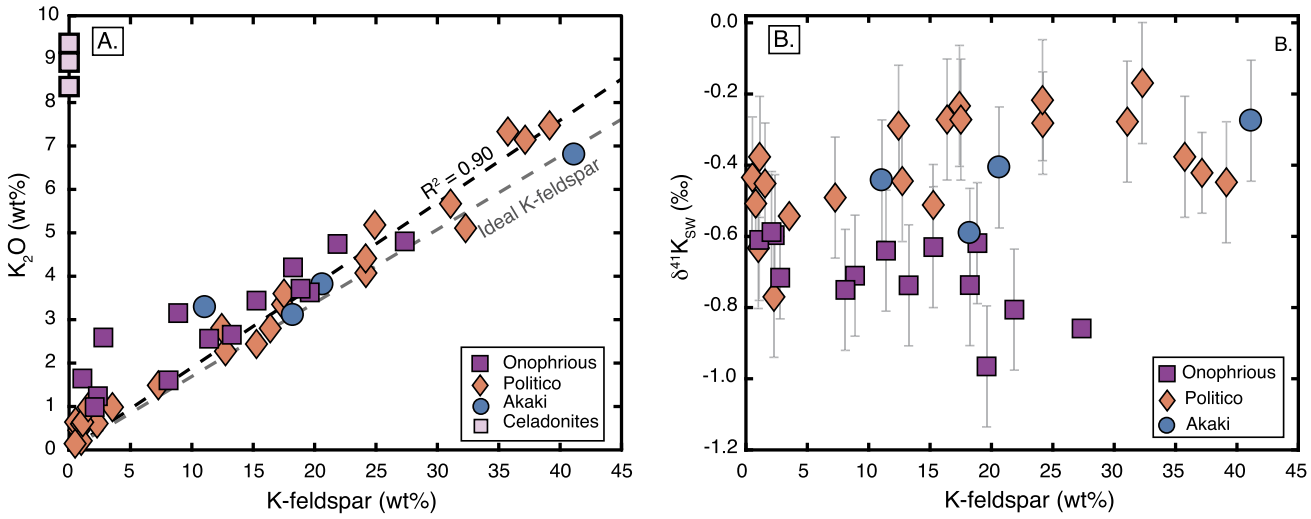

Fig. 6. K_2O content (A) and $\delta^{41}K$ (B) values as functions of K-feldspar abundance in Troodos samples. (A) Regression line through data has a similar slope to that expected for an "ideal" K-feldspar (17 wt% K_2O), suggesting that, for the samples analyzed here, K-feldspar is a major K-bearing mineral phase. Samples with high K_2O wt% despite low K-feldspar contents likely contain other K-rich secondary minerals (e.g. celadonite). (B) Cross-plot of $\delta^{41}K$ and K-feldspar content shows samples with similarly high K-feldspar abundance and markedly different $\delta^{41}K$ compositions, suggesting mineralogy cannot explain all the variability observed across Troodos sites.

Finally, the observed site-to-site variability in $\delta^{41}K$ and $\delta^{7}Li$ values in the Troodos ophiolite probably comes from the combined effects of mineralogy and diffusive vs. advective supply of K and Li. In turn, variations in these parameters result from differences in the history of sedimentation across these sites. We thus suggest that paired K and Li isotope measurements can be used as isotopic fingerprints for the study of low-temperature oceanic crust alteration.

Author contributions

D.S.R. and J.A.H. designed the project with input from L.A.C. D.S.R., J.A.H. and L.A.C. collected samples. D.S.R. performed laboratory work and J.G.M. assisted with Li isotope measurements. D.S.R. led manuscript writing with contributions from J.A.H., L.A.C. and J.G.M.

Declaration of competing interest

The authors declare that they have no known competing financial interests or personal relationships that could have appeared to influence the work reported in this paper.

Acknowledgements

The authors would like to acknowledge the Cyprus Crustal Study Project for making available some of the samples analyzed in this study (Akaki site). We also thank Rieko Adriaens for his help with quantitative XRD analysis. This project was funded through the Walbridge Fund Graduate Award to D.S.R. and NSF OCE CAREER grant #1654571 to J.A.H.

Appendix A. Supplementary material

Supplementary material related to this article can be found online at https://doi.org/10.1016/j.epsl.2020.116290.

References

Alt, J.C., Teagle, D.A., 1999. The uptake of carbon during alteration of ocean crust. Geochim. Cosmochim. Acta 63, 1527–1535.
Alt, J.C., Teagle, D.A., 2003. Hydrothermal alteration of upper oceanic crust formed at a fast-spreading ridge: mineral, chemical, and isotopic evidence from ODP Site 801. Chem. Geol. 201, 191–211.
Bednarz, U., Schmincke, H., 1989. Chemical patterns of sub-seafloor alteration and budget of mass transfer in the upper Troodos crust, Cyprus. Contrib. Mineral. Petrol. 102, 93–101.
Bourg, I.C., Richter, F.M., Christensen, J.N., Sposito, G., 2010. Isotopic mass dependence of metal cation diffusion coefficients in liquid water. Geochim. Cosmochim. Acta 74, 2249–2256.
Butterfield, D.A., Nelson, B.K., Wheat, C.G., Mottl, M.J., Roe, K.K., 2001. Evidence for basaltic Sr in midocean ridge-flank hydrothermal systems and implications for the global oceanic Sr isotope balance. Geochim. Cosmochim. Acta 65, 4141–4153.
Chen, H., Tian, Z., Tuller-Ross, B., Korotev, R.L., Wang, K., 2019. High-precision potassium isotopic analysis by MC-ICP-MS: an inter-laboratory comparison and refined K atomic weight. J. Anal. At. Spectrom. 34, 160–171.
Coogan, L.A., Daëron, M., Gillis, K., 2019. Seafloor weathering and the oxygen isotope ratio in seawater: insight from whole-rock $\delta^{18}O$ and carbonate $\delta^{18}O$ and Δ^{47} from the Troodos ophiolite. Earth Planet. Sci. Lett. 508, 41–50.
Coogan, L.A., Gillis, K.M., 2013. Evidence that low-temperature oceanic hydrothermal systems play an important role in the silicate-carbonate weathering cycle and long-term climate regulation. Geochem. Geophys. Geosyst. 14, 1771–1786.
Coogan, L.A., Gillis, K.M., 2018. Low-temperature alteration of the seafloor: impacts on ocean chemistry. Annu. Rev. Earth Planet. Sci. 46, 21–45.
Coogan, L., Gillis, K., Pope, M., Spence, J., 2017. The role of low-temperature (off-axis) alteration of the oceanic crust in the global Li-cycle: insights from the Troodos ophiolite. Geochim. Cosmochim. Acta 203, 201–215.
Demicco, R.V., Lowenstein, T.K., Hardie, L.A., Spencer, R.J., 2005. Model of seawater composition for the Phanerozoic. Geology 33, 877–880.
Dunlea, A.G., Murray, R.W., Santiago Ramos, D.P., Higgins, J.A., 2017. Cenozoic global cooling and increased seawater Mg/Ca via reduced reverse weathering. Nat. Commun. 8, 7. https://doi.org/10.1038/s41467-017-00853-5.
Elderfield, H., Schultz, A., 1996. Mid-ocean ridge hydrothermal fluxes and the chemical composition of the ocean. Annu. Rev. Earth Planet. Sci. 24 (1), 191–224.
Elderfield, H., Wheat, C., Mottl, M., Monnin, C., Spiro, B., 1999. Fluid and geochemical transport through oceanic crust: a transect across the eastern flank of the Juan de Fuca Ridge. Earth Planet. Sci. Lett. 172, 151–165.
Fantle, M.S., Higgins, J., 2014. The effects of diagenesis and dolomitization on Ca and Mg isotopes in marine platform carbonates: implications for the geochemical cycles of Ca and Mg. Geochim. Cosmochim. Acta 142, 458–481.
Farahat, N.X., Archer, D., Abbot, D.S., 2017. Validation of the BASALT model for simulating off-axis hydrothermal circulation in oceanic crust. J. Geophys. Res., Solid Earth 122, 5871–5889.
Fisk, M., Kelley, K.A., 2002. Probing the Pacific's oldest MORB glass: mantle chemistry and melting conditions during the birth of the Pacific Plate. Earth Planet. Sci. Lett. 202, 741–752.
Galy, A., Yoffe, O., Janney, P.E., Williams, R.W., Cloquet, C., Alard, O., Halicz, L., Wadhwa, M., Hutcheon, I.D., Ramon, E., et al., 2003. Magnesium isotope heterogeneity of the isotopic standard SRM980 and new reference materials for magnesium-isotope-ratio measurements. J. Anal. At. Spectrom. 18, 1352–1356.
Geske, A., Zorlu, J., Richter, D., Buhl, D., Niedermayr, A., Immenhauser, A., 2012. Impact of diagenesis and low grade metamorphosis on isotope ($\delta^{26}Mg$, $\delta^{13}C$, $\delta^{18}O$ and $^{87}Sr/^{86}Sr$) and elemental (Ca, Mg, Mn, Fe and Sr) signatures of Triassic sabkha dolomites. Chem. Geol. 332, 45–64.

Gillis, K., Coogan, L., Brant, C., 2015. The role of sedimentation history and lithology on fluid flow and reactions in off-axis hydrothermal systems: a perspective from the Troodos ophiolite. Chem. Geol. 414, 84–94.
Gillis, K., Robinson, P., 1991. Alteration of the ICRDG CY-1 and CY-1A drill cores, Troodos ophiolite: mineralogical and geochemical studies. In: Malpas, J., Robinson, P.T., Xenophontos, C. (Eds.), Cyprus Crustal Study Project: Initial Report, Holes CY-1 and CY-1A. In: Geological Survey of Canada, pp. 41–60. Paper 90-20.
Gothmann, A.M., Stolarski, J., Adkins, J.F., Higgins, J.A., 2017. A Cenozoic record of seawater Mg isotopes in well-preserved fossil corals. Geology 45, 1039–1042.
Hart, S.R., Staudigel, H., 1982. The control of alkalies and uranium in seawater by ocean crust alteration. Earth Planet. Sci. Lett. 58, 202–212.
Hauff, F., Hoernle, K., Schmidt, A., 2003. Sr-Nd-Pb composition of Mesozoic Pacific oceanic crust (site 1149 and 801, ODP Leg 185): implications for alteration of ocean crust and the input into the Izu-Bonin-Mariana subduction system. Geochem. Geophys. Geosyst. 4.
Higgins, J.A., Blättler, C., Lundstrom, E., Santiago-Ramos, D., Akhtar, A., Ahm, A.C., Bialik, O., Holmden, C., Bradbury, H., Murray, S., et al., 2018. Mineralogy, early marine diagenesis, and the chemistry of shallow-water carbonate sediments. Geochim. Cosmochim. Acta 220, 512–534.
Higgins, J.A., Schrag, D.P., 2010. Constraining magnesium cycling in marine sediments using magnesium isotopes. Geochim. Cosmochim. Acta 74, 5039–5053.
Higgins, J.A., Schrag, D.P., 2015. The Mg isotopic composition of Cenozoic seawater–evidence for a link between Mg-clays, seawater Mg/Ca, and climate. Earth Planet. Sci. Lett. 416, 73–81.
Hindshaw, R.S., Tosca, R., Goût, T.L., Farnan, I., Tosca, N.J., Tipper, E.T., 2019. Experimental constraints on Li isotope fractionation during clay formation. Geochim. Cosmochim. Acta 250, 219–237.
Horita, J., Zimmermann, H., Holland, H.D., 2002. Chemical evolution of seawater during the Phanerozoic: implications from the record of marine evaporites. Geochim. Cosmochim. Acta 66, 3733–3756.
Hu, Y., Chen, X.Y., Xu, Y.K., Teng, F.Z., 2018. High-precision analysis of potassium isotopes by HR-MC-ICPMS. Chem. Geol. 493, 100–108.
Huang, K.J., Teng, F.Z., Plank, T., Staudigel, H., Hu, Y., Bao, Z.Y., 2018. Magnesium isotopic composition of altered oceanic crust and the global Mg cycle. Geochim. Cosmochim. Acta 238, 357–373.
Husson, J.M., Higgins, J.A., Maloof, A.C., Schoene, B., 2015. Ca and Mg isotope constraints on the origin of Earth's deepest $\delta^{13}C$ excursion. Geochim. Cosmochim. Acta 160, 243–266.
James, R.H., Allen, D.E., Seyfried Jr., W., 2003. An experimental study of alteration of oceanic crust and terrigenous sediments at moderate temperatures (51 to 350 °C): insights as to chemical processes in near-shore ridge-flank hydrothermal systems. Geochim. Cosmochim. Acta 67, 681–691.
Kronberg, B., 1985. Weathering dynamics and geosphere mixing with reference to the potassium cycle. Phys. Earth Planet. Inter. 41, 125–132.
Kuhn, T., Versteegh, G., Villinger, H., Dohrmann, I., Heller, C., Koschinsky, A., Kaul, N., Ritter, S., Wegorzewski, A., Kasten, S., 2017. Widespread seawater circulation in 18–22 Ma oceanic crust: impact on heat flow and sediment geochemistry. Geology 45, 799–802.
Lauer, R.M., Fisher, A.T., Winslow, D.M., 2018. Three-dimensional models of hydrothermal circulation through a seamount network on fast-spreading crust. Earth Planet. Sci. Lett. 501, 138–151.
Li, W., Beard, B.L., Li, S., 2016. Precise measurement of stable potassium isotope ratios using a single focusing collision cell multi-collector ICP-MS. J. Anal. At. Spectrom. 31, 1023–1029.
Li, S., Li, W., Beard, B.L., Raymo, M.E., Wang, X., Chen, Y., Chen, J., 2019. K isotopes as a tracer for continental weathering and geological K cycling. Proc. Natl. Acad. Sci. 116, 8740–8745.
Lowenstein, T.K., Timofeeff, M.N., Brennan, S.T., Hardie, L.A., Demicco, R.V., 2001. Oscillations in Phanerozoic seawater chemistry: evidence from fluid inclusions. Science 294, 1086–1088.
Malpas, J., Williams, D., 1991. Geology of the area surrounding the CY-1 and CY-1A boreholes. In: Malpas, J., Robinson, P.T., Xenophontos, C. (Eds.), Cyprus Crustal Study Project: Initial Report, Holes CY-1 and CY-1A. In: Geological Survey of Canada, pp. 29–40. Paper 90-20.
McDuff, R.E., 1981. Major cation gradients in DSDP interstitial waters: the role of diffusive exchange between seawater and upper oceanic crust. Geochim. Cosmochim. Acta 45, 1705–1713.
Mewes, K., Mogollón, J.M., Picard, A., Rühlemann, C., Eisenhauer, A., Kuhn, T., Ziebis, W., Kasten, S., 2016. Diffusive transfer of oxygen from seamount basaltic crust into overlying sediments: an example from the Clarion–Clipperton fracture zone. Earth Planet. Sci. Lett. 433, 215–225.
Michalopoulos, P., Aller, R.C., 1995. Rapid clay mineral formation in Amazon Delta sediments: reverse weathering and oceanic elemental cycles. Science 270, 614–617.
Millot, R., Guerrot, C., Vigier, N., 2004. Accurate and high-precision measurement of lithium isotopes in two reference materials by MC-ICP-MS. Geostand. Geoanal. Res. 28, 153–159.
Misra, S., Froelich, P.N., 2012. Lithium isotope history of Cenozoic seawater: changes in silicate weathering and reverse weathering. Science 335, 818–823. https://doi.org/10.1126/science.1214697.
Moores, E., Robinson, P.T., Malpas, J., Xenophonotos, C., 1984. Model for the origin of the Troodos massif, Cyprus, and other mideast ophiolites. Geology 12, 500–503.
Morgan, L.E., Santiago Ramos, D.P., Lloyd, N.S., Higgins, J.A., 2018. High precision $^{41}K/^{39}K$ measurements by MC-ICP-MS indicate terrestrial variability of $\delta^{41}K$. J. Anal. At. Spectrom. https://doi.org/10.1039/C7JA00257B.
Parendo, C.A., Jacobsen, S.B., Wang, K., 2017. K isotopes as a tracer of seafloor hydrothermal alteration. Proc. Natl. Acad. Sci. 114, 1827–1831.
Plank, T., Ludden, J., Escutia, C., Party, S., 2000. Leg 185 summary: inputs to the Izu–Mariana subduction system. Proc. Ocean Drill. Program, Initial Rep., 1–63. Leg 185.
Pogge Von Strandmann, P.A., Jenkyns, H.C., Woodfine, R.G., 2013. Lithium isotope evidence for enhanced weathering during Oceanic Anoxic Event 2. Nat. Geosci. 6, 668–672.
Rautenschlein, M., 1987. Geology and geochemistry of Akaki volcanics, Cyprus. PhD thesis. Ruhr-Universität Bochum.
Regelous, M., Haase, K., Freund, S., Keith, M., Weinzierl, C., Beier, C., Brandl, P.A., Endres, T., Schmidt, H., 2014. Formation of the Troodos ophiolite at a triple junction: evidence from trace elements in volcanic glass. Chem. Geol. 386, 66–79.
Richter, F.M., Mendybaev, R.A., Christensen, J.N., Hutcheon, I.D., Williams, R.W., Sturchio, N.C., Beloso Jr., A.D., 2006. Kinetic isotopic fractionation during diffusion of ionic species in water. Geochim. Cosmochim. Acta 70, 277–289.
Santiago Ramos, D.P., Morgan, L.E., Lloyd, N.S., Higgins, J.A., 2018. Reverse weathering in marine sediments and the geochemical cycle of potassium in seawater: insights from the K isotopic composition ($^{41}K/^{39}K$) of deep-sea pore-fluids. Geochim. Cosmochim. Acta 236, 99–120.
Seyfried, W., Bischoff, J., 1979. Low temperature basalt alteration by sea water: an experimental study at 70 °C and 150 °C. Geochim. Cosmochim. Acta 43, 1937–1947.
Shalev, N., Bontognali, T.R., Wheat, C.G., Vance, D., 2019. New isotope constraints on the Mg oceanic budget point to cryptic modern dolomite formation. Nat. Commun. 10, 1–10.
Spencer, R., Hardie, L., 1990. Control of seawater composition by mixing of river waters and mid-ocean ridge hydrothermal brines. In: Spencer, R.J., Chou, I.M. (Eds.), Fluid Mineral Interactions: A Tribute to H.P. Eugster. In: Geochem. Soc. Spec. Publ., vol. 2, pp. 409–419.
Teng, F.Z., 2017. Magnesium isotope geochemistry. Rev. Mineral. Geochem. 82, 219–287.
Tomascak, P.B., Langmuir, C.H., le Roux, P.J., Shirey, S.B., 2008. Lithium isotopes in global mid-ocean ridge basalts. Geochim. Cosmochim. Acta 72, 1626–1637.
Wang, K., Jacobsen, S.B., 2016. An estimate of the Bulk Silicate Earth potassium isotopic composition based on MC-ICPMS measurements of basalts. Geochim. Cosmochim. Acta 178, 223–232.
Weis, D., Kieffer, B., Maerschalk, C., Barling, J., De Jong, J., Williams, G.A., Hanano, D., Pretorius, W., Mattielli, N., Scoates, J.S., et al., 2006. High-precision isotopic characterization of USGS reference materials by TIMS and MC-ICP-MS. Geochem. Geophys. Geosyst. 7.
Wheat, C.G., Fisher, A.T., 2008. Massive, low-temperature hydrothermal flow from a basaltic outcrop on 23 Ma seafloor of the Cocos Plate: chemical constraints and implications. Geochem. Geophys. Geosyst. 9.
Wheat, C.G., Mottl, M.J., 2000. Composition of pore and spring waters from Baby Bare: global implications of geochemical fluxes from a ridge flank hydrothermal system. Geochim. Cosmochim. Acta 64, 629–642.
Wimpenny, J., Colla, C.A., Yin, Q.Z., Rustad, J.R., Casey, W.H., 2014. Investigating the behaviour of Mg isotopes during the formation of clay minerals. Geochim. Cosmochim. Acta 128, 178–194.